



## Measurement of electron temperature of Topside ionosphere: A review

Koh-ichiro Oyama <sup>1,2</sup>

<sup>1</sup>National Cheng Kung University, No 1. Ta-Sheuh Road, Taian, Taiwan

<sup>2</sup>A Hokkaido University, Sapporo Japan

### Abstract

This discourse is part of a review work that encompasses the basic aspects of satellite insitu probe in measurement of electron temperature  $T_e$  and density  $N_e$ . A few limitations of such techniques in delivering accurate  $T_e$  values are presented along with suggestions' for their improvement. The diurnal, latitudinal, and longitudinal variations of  $T_e/N_e$  in the equatorial ionosphere at F-layer height are shown, finally to identify the modifications in  $T_e$  in presence of plasma bubbles. The role of neutral wind and associated physics are brought in to the discussion in relevance to imprinted features in  $T_e$  and  $N_e$ . The part (b) of the review work will cover effects of geomagnetic disturbances in electron temperature and in the consequent effect in space weather relation.

*Key words: Electron temperature: satellite probes: F-layer density; plasma bubbles; neutral wind*

### 1. Introduction

The purpose of the paper is to show the results which is obtained with an electron temperature ( $T_e$ ) robe developed in Japan in the year 1970. The discussion will be based on the instrumentation and result obtained with this probe onboard in Japanese satellites. We show two satellite results; one is Hinotori which measured low latitude region at the height of 600km, another one is Akebono which measure electron temperature up to the height of 800km in low / mid latitudes.

One major factor to measure  $T_e$  accurately in the topside ionosphere and plasma sphere is electrode contamination. Recently two satellites, CHAMP and DEMETER were launched for monitoring parameters in the F and topside ionosphere. Both two satellites accommodate Dc Langmuir probe. The paper published by Lebreton et al., 2006, surely shows the hysteresis of current-voltage ( $v-i$ ) curve i.e.,



the probe current takes different paths for increasing and decreasing biases of the sweep voltage. We believe that this is generated by the contamination over the electrode.  $T_e$  is around 3000-4000 K for daytime, and  $T_e$  during the night time is much higher than neutral temperature. Usually  $T_e$  is very close to neutral temperature at night. If the value obtained by DEMETER is right, there is a possibility that  $T_e$  during extremely low solar activity is higher than that during higher solar flux period. However even we accept this assumption, the value seems to be still very high.

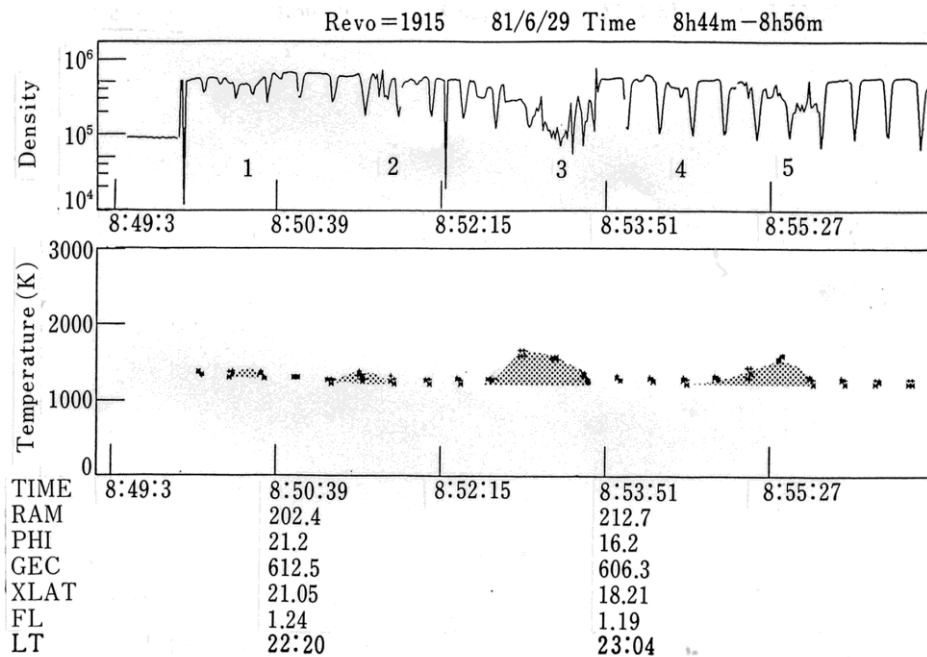
Frequency response of the amplifier is not so serious compared with Lower E region  $T_e$  measurement because  $T_e$  in the topside ionosphere is at least 4-5 times higher than that in the lower E region. Attention needs to be paid on sampling rate of the data. Number of the sampling of the data in the electron retardation range should be at least 10 samples for curve fitting. Otherwise, electron temperature is overestimated. This situation seems to appear for the satellite CHAMP. DC probe onboard the CHAMP satellite seems to have insufficient sampling number at night in the  $T_e$  determination region as long as we examine the raw data shown by Cooke (2003).  $T_e$  measurement by CHAMP during night time is sometimes overestimated (Private Communication).  $T_e$  values in the time period from 2000 to 0300 hrs LT during March equinox show about 500K higher than HINOTORI satellite data (Oyama et al., 1996; Su et al., 1995; Su et al., 1996; Balan et al., 1997).  $T_e$  observed by Japanese satellite "HINOTORI2 has been well accepted as a reference amongst ionosphere community.  $T_e$  observed by CHAMP in December equinox is about 400K higher than that of HINOTORI. During day time HINOTORI and CHAMP data show quite good agreement for all March and September equinox, June and December solstice. IRI shows a good agreement with HINOTORI data during night time.  $T_e$  of IRI should be close to the true value because at these altitudes, electron temperature is nearly equal to neutral temperature. We presume that this high temperature observed by CHAMP could be possibly evaluated from the lack of sampling rate (Cooke et al., 2003); sampling of number in the electron retarding region is some times only three or four points during night time, where electron density is low. If we fit the curve to the small number of observed data points, the slope of the curve is milder than the true case, which provides  $T_e$  higher than the true value.

In Japan a resonance rectification probe has also been accommodated in 5 earth orbiting satellite. The probe was accommodated in Korean satellite as well as in Brazilian satellite. The probe was also placed in Mars orbiter which unfortunately disconnected the radio signal from the orbiter (Oyama et al., 1999).

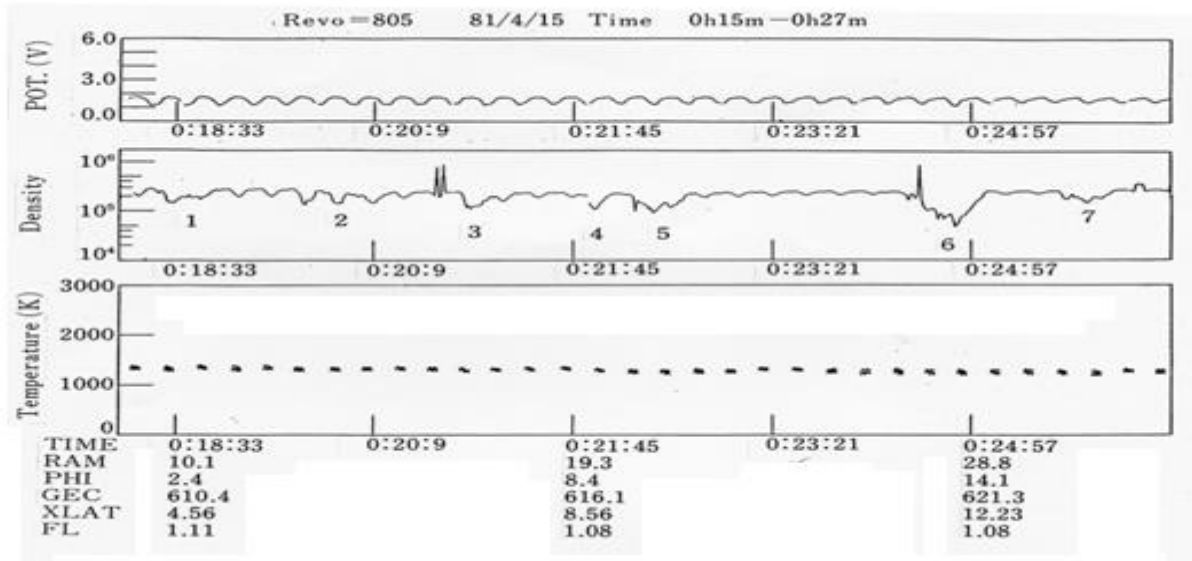


**1.1 Te in the Plasma bubble**

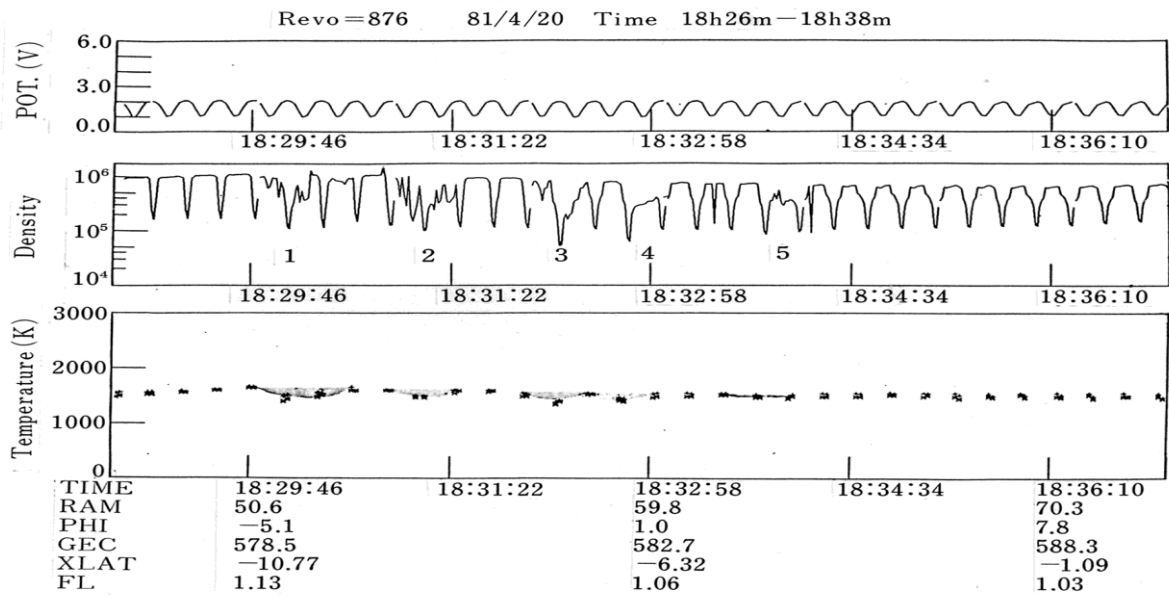
Satellite `HINOTORI` which was in the orbit with an inclination of 31° at the height of 600km. During the short mission period from February 1981 to July 1982, Te was measured with Ne (electron density) when the data recorder was used to store one satellite orbit data. As the purpose of Hinotori satellite is to pick up the flare phenomena, data recorder was occupied by solar flare related instrument for transient phenomena. Therefore Te and Ne data were stored only when no flare is recorded. As the storing capability of the recorder is only one orbit data, the number of the pass which can be retrieved is limited to the region where we could receive the signal from Kagoshima Space Center. As a result the number of the satellite pass is about 3-4 in numbers. Hinotori conducted the first systematic measurement of Te in the plasma bubble at the height of 600 km. The electron temperature in the plasma bubble shows higher, lower and equal values with respect to the ambient as shown in Figure 1.



(a)



(b)



(c)

Figure 1. Three features of Te inside plasma bubble. (a) Te is higher than ambient; (b) Te is the same as ambient and (C) Te is lower than the ambient.

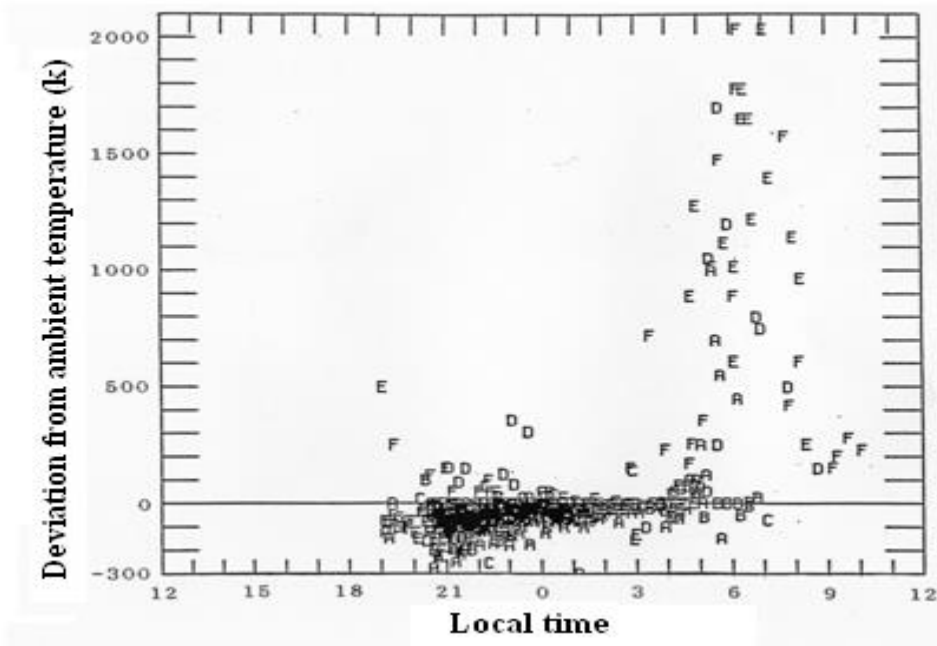


Figure 2. Local time variation of  $T_e$  in plasma bubble The symbols define the longitude sectors :  
 A=0-59 ; B=60-119; C=120-179 ; D=180-239 ; E=240-299 ; F=300-359

The different features of  $T_e$  inside plasma bubble are understood as the local time variation. As Figure 2 shows that before mid night  $T_e$  in the bubble displays lower value than  $T_e$  outside. It gradually approaches the outside temperature and equal to ambient  $T_e$  at around 0300 LT, and after 0300 LT,  $T_e$  inside plasma bubble starts to increase. The low  $T_e$  before mid night can be explained as follows.  $T_e$  which rises fast still keeps the  $T_e$  of lower height, and therefore  $T_e$  in the bubble is lower than ambient. After midnight,  $T_e$  becomes equal to the ambient, which means that heats propagate across plasma wall and heat the electrons in side plasma bubble. Finally  $T_e$  becomes higher than the ambient. At this stage photoelectrons from outside reached plasma inside along the magnetic field. In the morning,  $T_e$  starts to reach the ambient; which corresponds to the disappearance of the bubble.

Figure 3 shows two successive behavior of  $T_e$  in the plasma bubble which appeared just before sunrise at 7:55:35. For Rev 482, inside the bubble,  $T_e$  is slightly higher than ambient, and for 483, the bubble develops and  $T_e$  reaches about 4500 K.

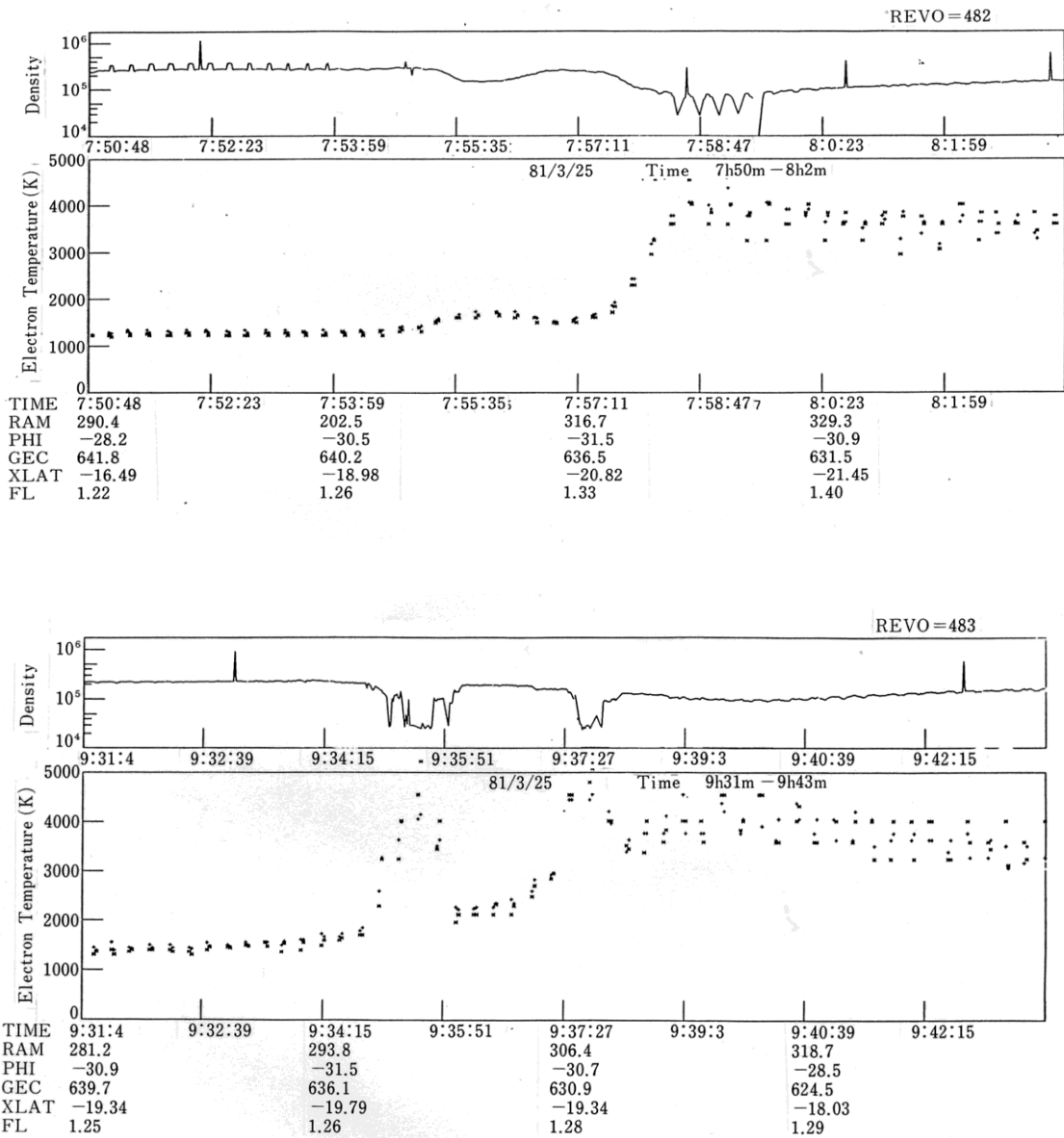


Figure 3. Te of two successive bubbles in the early morning

As Figure 2 shows, there are a few cases where Te is higher than ambient at the time when Te should be lower than ambient. Figure 4. illustrates the location where Te is higher than the ambient temperature. It is found that elevated Te first occurs in South Atlantic Anomaly. Other location of Te elevation occurs in the Hawaiian anomaly where Japanese X astronomy group found the strong charged particle precipitation.

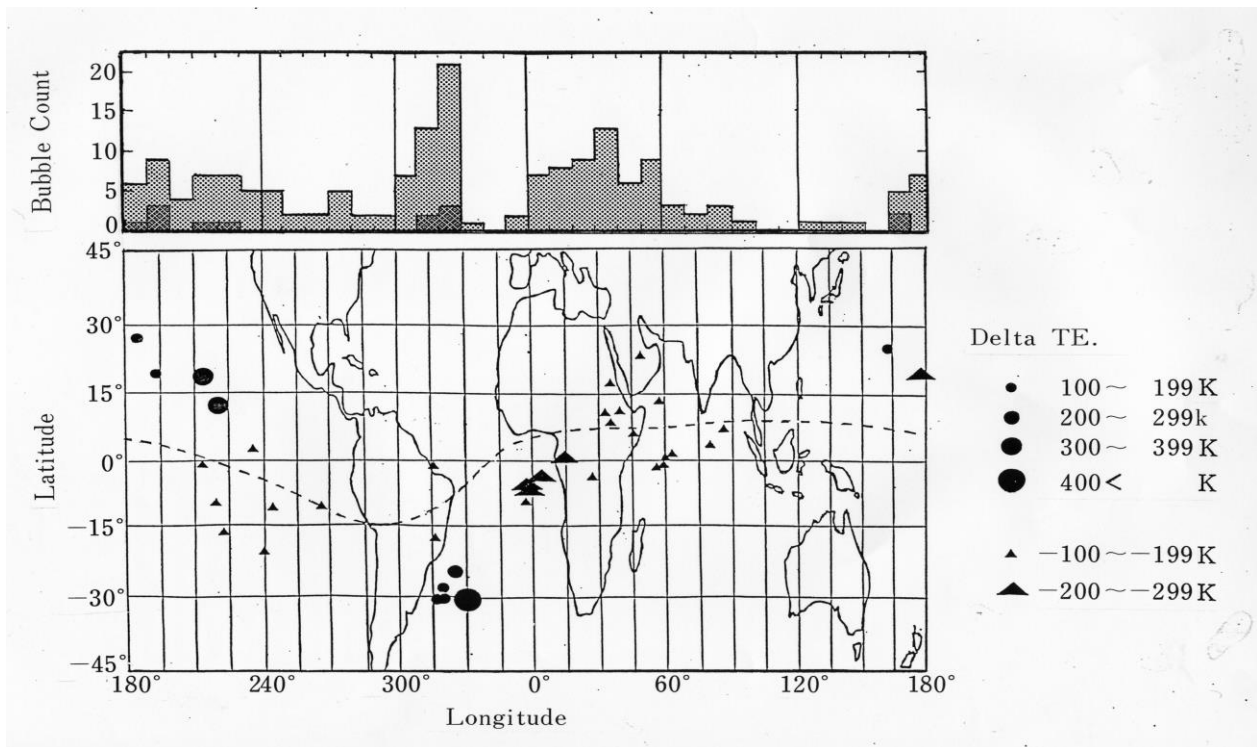


Figure 4. Location of high Te. Top panel; Grey code shows the total number of the bubble, while black shows the number of the bubble in which higher Te is observed.

In future, more detailed structure of Te around plasma bubble should be measured as the horizontal resolution of our results was not enough to discuss Te in the edge of plasma bubble. To get Te around plasma bubble, data process system to generate Te from raw v-I curve needs to be easy. We found that Te at the edge is higher than the ambient sometimes. The result might be applied to calculate heat input to 600km which is not still fully successful.

### ***1.2 Dynamics of topside ionosphere***

The Ne/Te data which were obtained by Hinotori turned out to be the most beautiful data set at the height of 600 km and many papers have been published [Watanabe and Oya, 1986; Takahashi et al, 1987; Oyama and Schlegel 1988; Schlegel et al., 1989; Oyama 1991, 1994; Oyama et al., 1993, 1996a; Watanabe et al., 1995a ; Su et al, 1995, 1996a, 1996b; Balan, 1997,Dabas et al., 2000].



In 1996, we had reported longitudinal variation of Te alone. In this paper we describe features of both Te and Ne at two different longitude zones for three seasons in order to show the significant role of both zonal and meridional winds. Data for these three seasons are equinox (February, March, April in 1981 and 1982, September and October in 1981, denoted as E.Q.X hereafter) summer in the northern hemisphere (May, June in 1981 and 1982, and July in 1981, denoted as M.J.J hereafter), and summer in the southern hemisphere (November, December and January, denoted as N.D.J hereafter). The results which are summarized here are expected to contribute to the revision of the IRI of Te/Ne and to serve as a reference to other Te/Ne observations at the height of 600 km in the equatorial region ( within 30 degrees in geomagnetic latitudes). The results can also be used for educational purpose because they show very clear and ideal neutral wind effects on the topside ionosphere. In chapters 2, 3, and 4, data which are processed irrespective of solar flux F10.7 are used because the number of the data otherwise becomes insufficient for the discussion. However brief description is given about the solar flux dependence in chapter 5, because the effect of solar flux intensity F10.7 can be seen in spite of the small range of the solar activity variation during the satellite observation.

## **2. Local time variation of Ne at three seasons in two longitude zones**

Figures 1a,1b,and 1c show the local time variation of Ne for three seasons for the longitude zone of 210-285 degrees where magnetic meridional plane tilts about maximum 10 degrees toward east. Ne values which are plotted in the figure are the data averaged during individual 3 seasons. One feature which is common to all three figures is that Ne takes minimum value around 4 local time which is right before sunrise, increases toward daytime, and finally reduces in the evening.

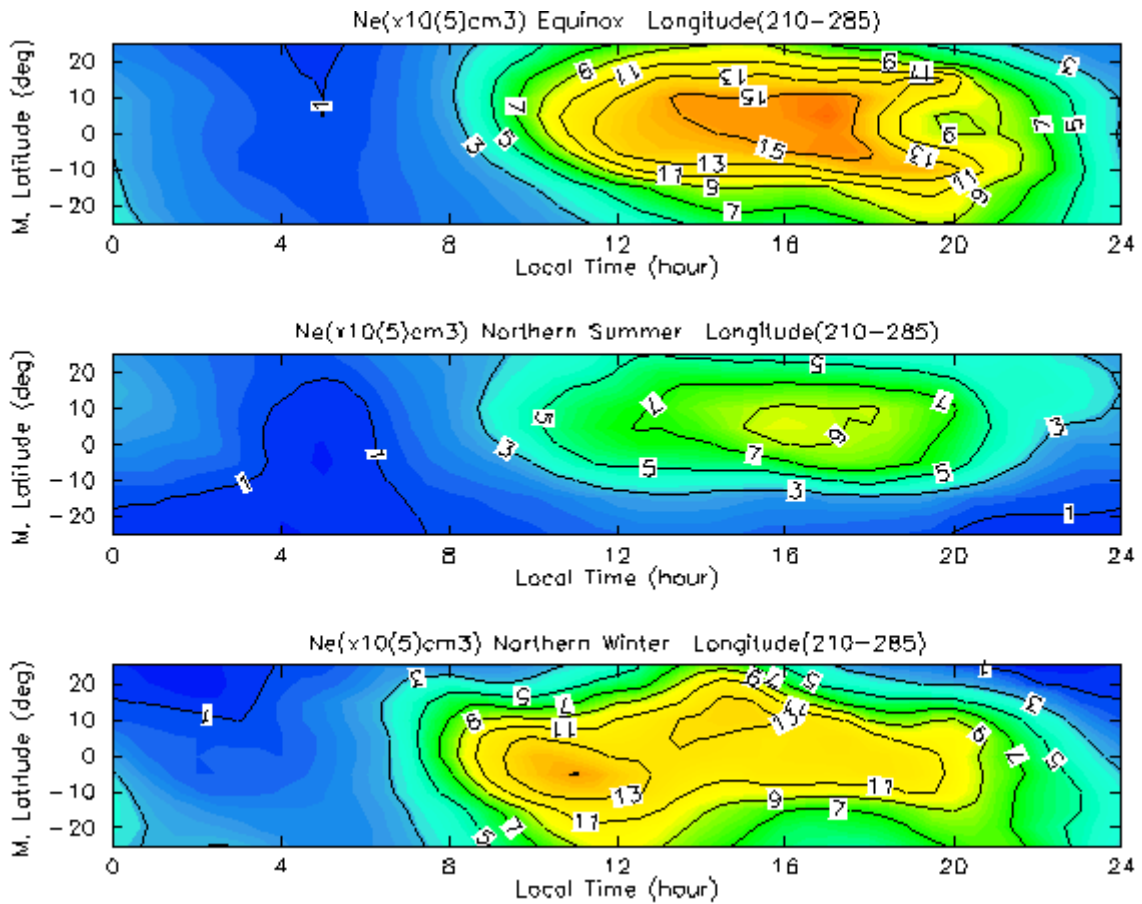


Figure 5. Local time variation of Ne for three seasons; (a) equinox, (b) summer in northern hemisphere and (c) winter in northern hemisphere for the longitude zone of 210-285.

It is noted in these figures that two equator clefts of both hemispheres are smeared out as a result of averaging many satellite passes.

During the equinox (upper panel) when wind blows toward high latitudes, local time variation is roughly symmetric in the northern and southern hemispheres. It is, however, noted that Ne around 7-11 LT is higher in the northern hemisphere than in the southern hemisphere and higher in the southern hemisphere than in the northern hemisphere around 17-20 LT. During northern summer season (middle panel), Ne in the northern hemisphere is higher than in the southern hemisphere.

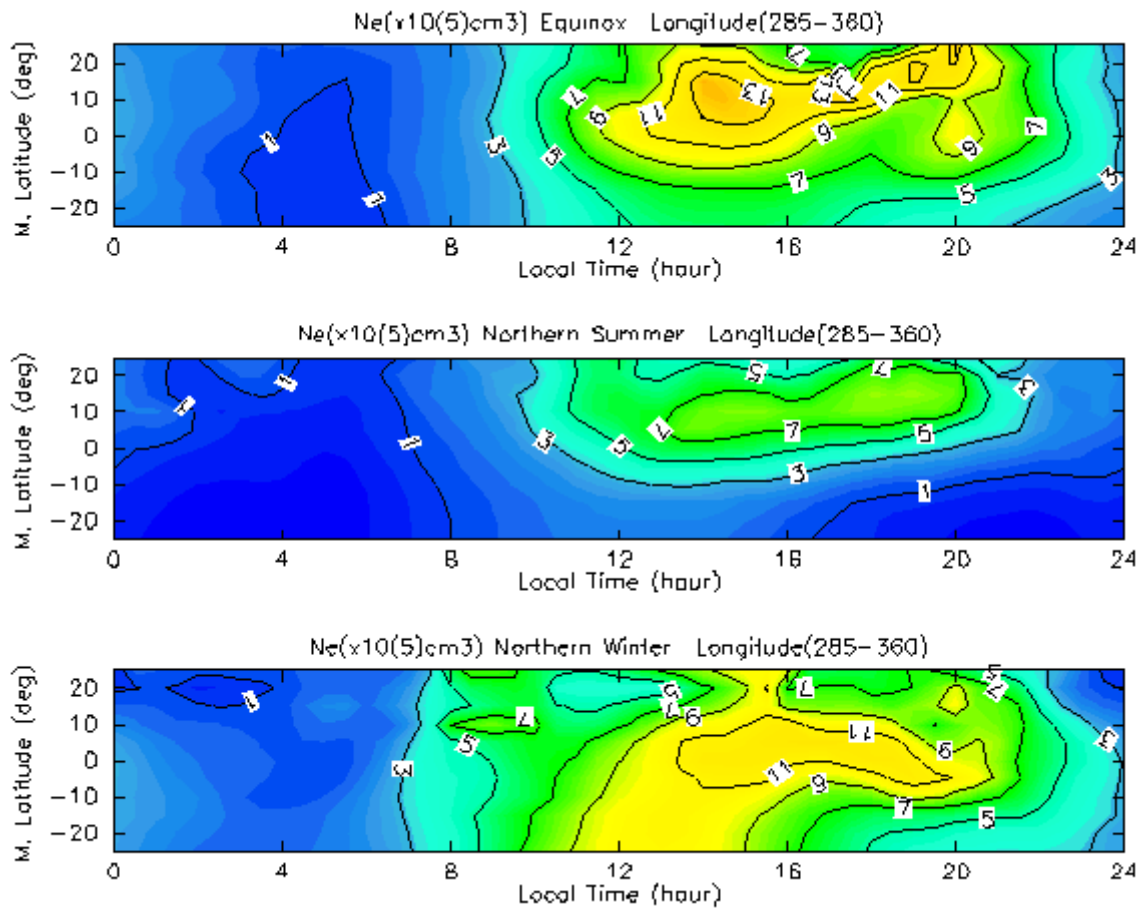


Figure 6. Same as Figure 1 but for the longitude zone of 285-360

Whilst in northern winter, Ne in the southern hemisphere is higher than in the northern hemisphere. Among the three panels, Ne is the lowest in northern summer, which shows the seasonal anomaly.

In Figures 6a, 6b, and 6c Ne profiles are shown for the longitude zone of 285-360, where magnetic meridional plane tilts westwards by about a maximum of 20 degrees. General behavior of Ne in this latitude zone is nearly the same as for 210-285, but a clear difference exists between two longitude zones. For example Figure 6a (equinox) Ne in the southern hemisphere is higher than in the northern hemisphere and in the afternoon Ne in the northern hemisphere is higher than in the southern hemisphere, which is the opposite to the Figure 5a. This is attributed to the difference of the declination of the magnetic meridional plane in two longitude zones. Another factor for the difference of Ne might be due to the difference of neutral wind velocity at two different longitudes. The difference between two longitude zones can be recognized more clearly in Te behavior than Ne as we show later.



Ne at Morning overshoot of Te

Season	210-285		285-360	
	North	South	North	South
M.J.J	5.22-5.35	5.02-5.04 an	4.91-5.19	4.81-5.03 bn
N.D.J	5.31-5.41	5.36-5.51 cn	5.25-5.59	5.38-5.58 dn
E.Q.X	5.11-5.34	5.17-5.24 en	5.18-5.22	5.07-5.25 fn

Ne at Afternoon overshoot of Te

Season	210-285		285-360	
	North	South	North	South
M.J.J	5.62-5.65	5.13-5.16 gn	5.57-5.85	4.90-5.03 hn
N.D.J	5.66-5.40	5.72-5.76 in	5.79-5.84	5.73-5.86 jn
E.Q.X	5.81-5.91	5.81-5.90 kn	5.76-5.81	5.69-5.78 ln

Table 1. Log10Ne at the morning overshoot and afternoon overshoot. Ne are the values during morning overshoot between 6-7:30 LT and during the afternoon overshoot between 16:30-18:00 LT at the geomagnetic latitudes of 20 degrees in both hemispheres. Boxes where both zonal and meridional wind components are enhanced are surrounded by thick line

Table 1 summarizes typical Ne values in both hemispheres, where Ne at morning overshoot of Te as well as at afternoon overshoot (see next paragraph) are listed for the two longitude zones of 210-285 degrees and 285-360 degrees for three seasons. These values are taken from Research Note (Watanabe et.al., 1995b; Oyama et al., 1994). Two boxes which are surrounded with thick line (marked as **an** and **dn** for the morning overshoot and **hn** and **in** for the afternoon overshoot) are the cases where both zonal and meridional winds drive plasma to the same direction along magnetic line of force and as a result the effect of two winds is enhanced as we describe in section 3. Other boxes (marked as **bn**, **cn**, **en**, and **fn** for the morning overshoot and **gn**, **jn**, **kn**, and **ln** for the afternoon overshoot in the boxes at the right end of the boxes) are the cases where zonal and meridional wind components weaken their effect each other.

### 3. Local time variation of Te at two longitude zones 210-285 and 285-360 degrees.

Figures 6a, 6b, and 6c show local time variation of Te for three seasons for the longitude zone of 210-285 degrees corresponding to Ne shown in Figures 4a, 4b, and 4c.

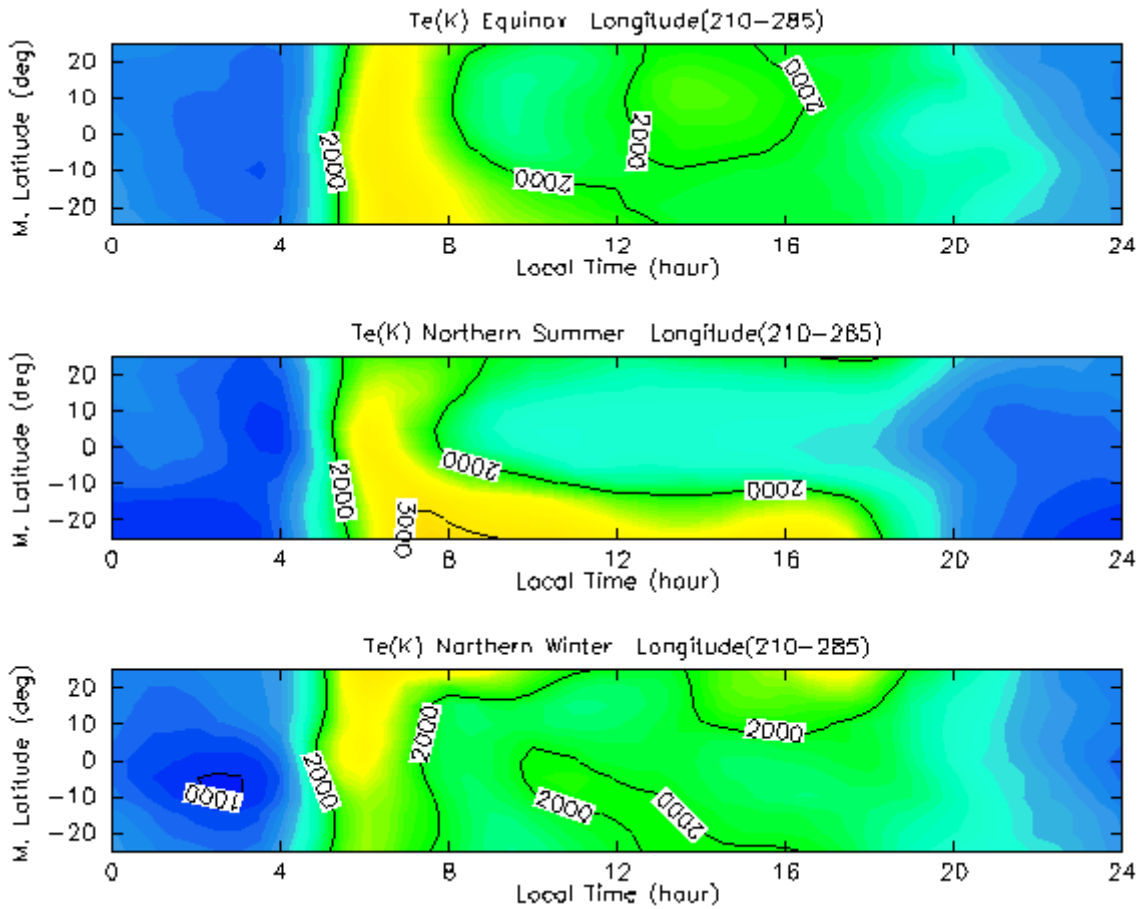


Figure 6. Local time variation of  $T_e$  for the longitude zone of 210-285;(a) equinox,(b) summer in northern hemisphere, and ( c) winter in northern hemisphere

General features of local time variation of  $T_e$  are as followings.  $T_e$  shows the lowest value around 4:00 LT, rising steeply, and takes the peak value at about 6 LT (which is, well known "morning overshoot"). After the morning overshoot,  $T_e$  decreases, and again takes the high value around 16 LT; the peak value increases as we move to the higher latitude (hereafter, we call "afternoon overshoot"). As shown in Figure 6a (equinox), high  $T_e$  region in the northern hemisphere is smaller than in the southern hemispheres. In the northern summer (Figure 6b), there is a single peak in northern hemisphere and an extended period (06LT to 18 LT) of high temperature in the southern hemisphere, whereas in the northern winter (Figure 6c) there appears to be two peaks in the northern hemisphere and only one in the southern hemisphere.

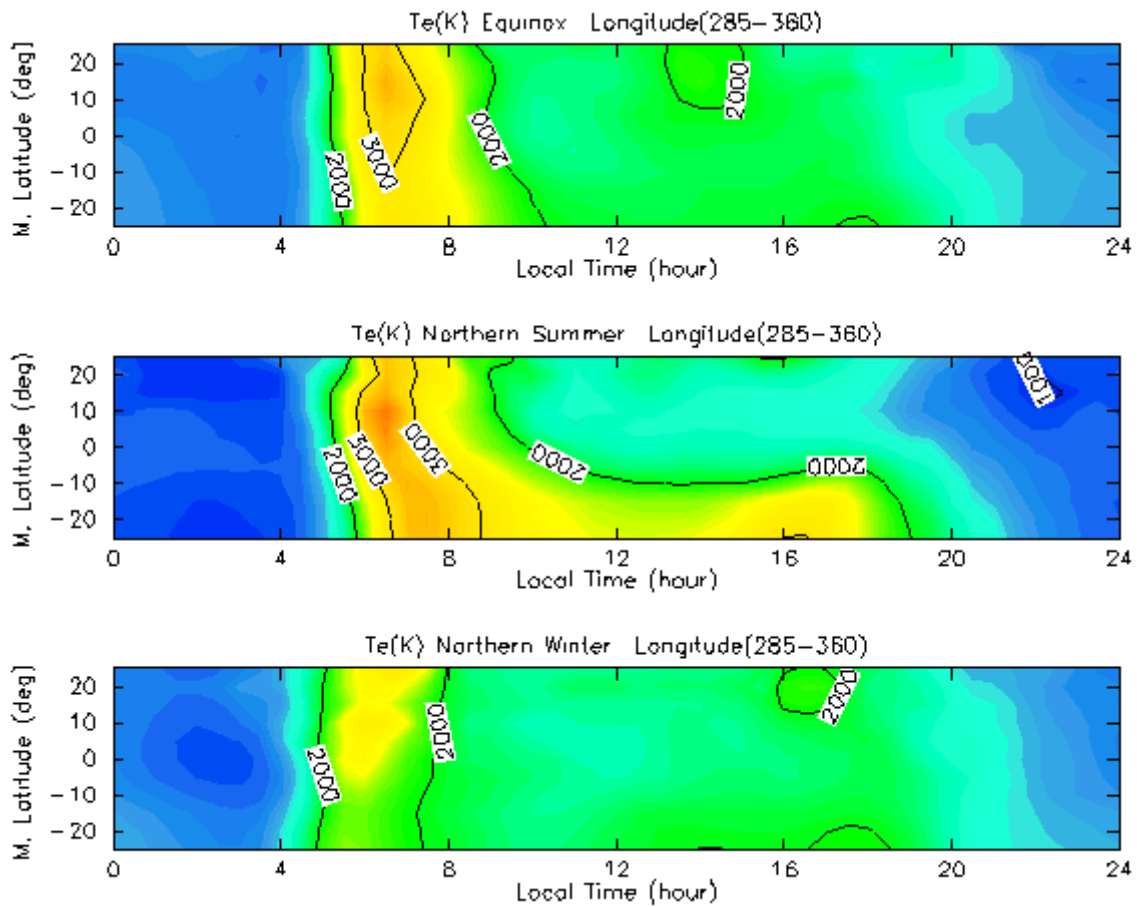


Figure 7. Same as Figure 3 but for the longitude 285-360

Figures 7a, 7b, and 7c show  $T_e$  in the same format as for Figure 6 for three seasons but in the longitude zone of 285-360, corresponding to the  $N_e$  behaviors which are shown in Figures 5a, 5b, and 5c. Although the gross features are same as for the longitude zone of 210 - 285 degrees, a slight, but still geophysically meaningful difference of  $T_e$  exists between two longitude zones.  $T_e$  at the morning overshoot as well as afternoon overshoot as typical examples of the difference are summarized in table 2 for two longitude zones and for three seasons. Similar to table 1, boxes which are surrounded by thick line (marked as **at** and **dt** for the morning overshoot and **it** and **ht** for the afternoon overshoot at the end of the boxes) indicates the cases where both meridional and zonal wind components drive plasma to the same direction and consequently two effects is enhanced, while other boxes (marked as **bt**, **ct**, **et**, and **ft** for the morning overshoot and **gt**, **jt**, **kt** and **lt** for the afternoon overshoot in the boxes ) show the cases where two wind components suppress the effects each other.



Te (K) at Morning overshoot

Season	210-285		285-360	
	North	South	North	South
M.J.J	2170	3140 at	3250	3300 bt
N.D.J	2960	2320 ct	2950	2290 dt
E.Q.X	2630	2860 et	3200	2900 ft

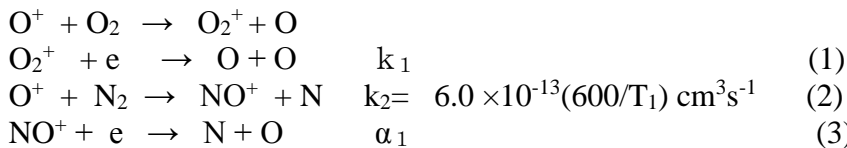
Te(K) at Afternoon overshoot

Season	210-285		285-360	
	North	South	North	South
M.J.J	2070	2870 gt	2040	3010 ht
N.D.J	2650	2000 it	2050	2040 jt
E.Q.X	2020	1990 kt	1900	2030 lt

Table 2. Te at morning overshoot and afternoon overshoot at two longitude zones. Columns surrounded by thick lines indicate that both zonal and meridional winds drive plasma in the same direction and as a result the effect of two winds is enhanced.

#### 4. Effect of neutral wind on Ne / Te

Basic chemical reactions which are working in the topside ionosphere are:



Detail value of  $\alpha_1$  is given by M.Torr and D. Torr (1979) and roughly is expressed as  $\alpha_1 = (4.3) \times 10^{-7} (\text{Te}/300)^{-0.83} \text{ cm}^3\text{s}^{-1}$ . The features of Ne which appeared in Figures 4a, 4b, and 4c and 5a, 5b, and 5c can be well explained by the effects of neutral wind which blows at the height which we are discussing. Major effect is produced by meridional wind component, which generates the difference between two hemispheres depending on seasons, while zonal wind component produces the difference between two longitude zones. Figure 8 shows schematic picture on the effect of meridional wind components on the plasma motion, (a) winter in northern hemisphere, (b) equinox, and (c) summer in northern hemisphere.

In the Figure 8,  $B$  is an earth magnetic field.  $V_M$  is the horizontal wind component in the wetward tilted magnetic meridian plane.  $V_{BM}$  is the velocity component along the geomagnetic line force.

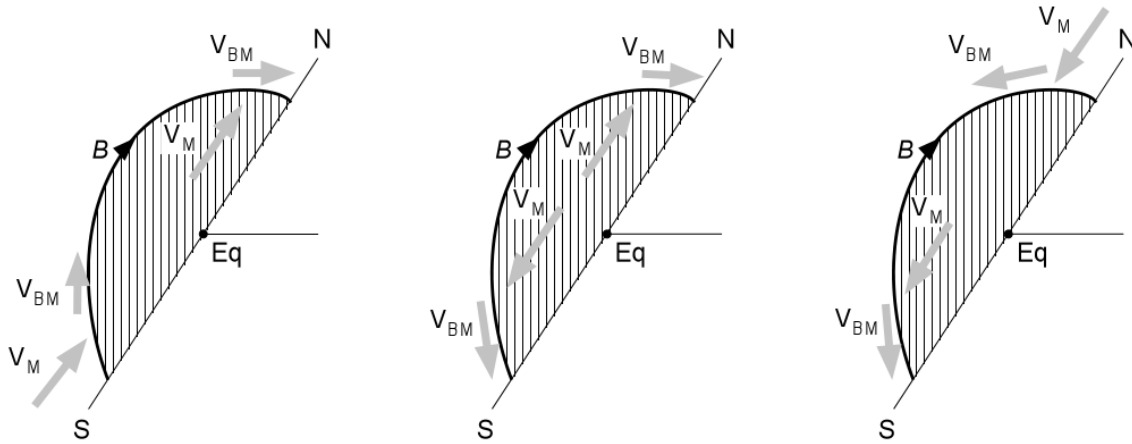


Figure.8. Effect of the meridional wind on the electron density increase/decrease in the topside ionosphere: (a) northern winter, (b) equinox, and (c) northern summer. Arrows indicate the direction of neutral wind  $V_M$  and plasma drift  $V_{BM}$  along geomagnetic line of force.

In the following we discuss the effect of meridional and zonal winds following the treatment of Hedin et al., (1991) for wind system in 10-30 degrees latitude. For northern summer season when the neutral wind blows from the northern hemisphere to the southern hemisphere as shown in Figure 5a, the ions are pushed up to the high altitude in the northern hemisphere along the magnetic line of force by the force which is generated as a result of the collision between ions and neutral particles. Consequently, recombination of neutral nitrogen reduces and as a result electron density increases because recombination of the reactions (2) and (3) is less. Whilst in the southern hemisphere, ions are pushed down along the geomagnetic line of force, and as the result electron density decreases because the reactions (2) and (3) becomes more effective.

In the northern winter hemisphere, ions are pushed up in the southern hemisphere and pushed down in the northern hemisphere and consequently electron density increases in the southern hemisphere and decreases in the northern hemisphere.

In addition to the meridional wind effect, zonal wind influences on the behaviors of plasma density.

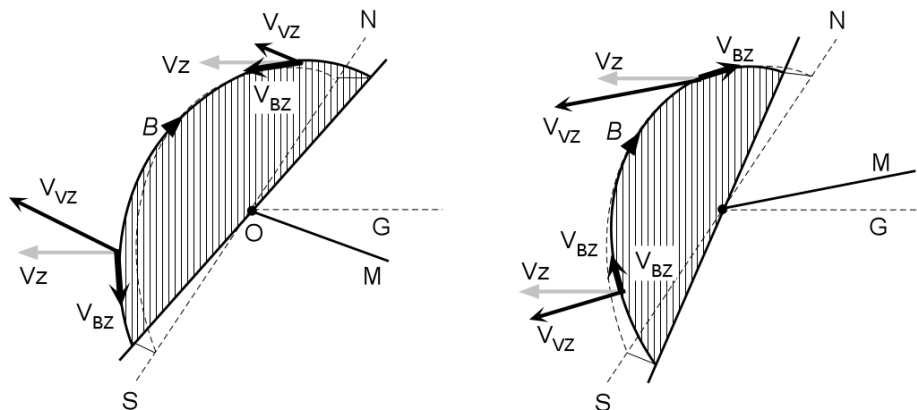


Figure 9. Effect of the declining magnetic meridional plane caused by zonal wind in the morning at two different longitude zones (a) longitude 210-285, and (b) longitude 285-360.

Figure 9 a and b show the effect of tilting angle of the magnetic meridional plane, where  $V_z$  is the zonal wind velocity,  $V_{vz}$  is the component of zonal wind  $V_z$ , which is vertical to the magnetic meridional plane and  $V_{bz}$  along the magnetic field line, respectively. When the neutral wind blows westward (that is, from east to west) in the early morning in the Asian sector where magnetic meridional plane tilts toward eastward as shown in Figure 9a, ions are pushed up in the northern hemisphere and pushed down in the southern hemisphere. By the same chemical reactions as mentioned for meridional wind component, electron density increases in the northern hemisphere and reduces in the southern hemisphere. When the wind blows eastward (that is, from west to east), ions are pushed up in the southern hemisphere and pushed down in the northern hemisphere. Consequently electron density increases in the southern hemisphere and reduces in the northern hemisphere.

Magnetic meridional plane tilts toward westward in the latitude range of 285-360. When wind blows westward in the morning as shown in Figure 6b, ions are pushed down in the northern hemisphere and pushed up in the southern hemisphere. Consequently electron density increases in the southern hemisphere and reduces in the northern hemisphere. When the wind blows eastward in the afternoon, electron density changes are just the other way.

In order to summarize the description above, the combined effects of zonal and meridional winds for two different longitude zones is tabulated in Table 3.

Morning



Hemisp. Season	210~285		285~360	
	North	South	North	South
M.J.J	▲    △	▼    ▽ ad	▲    ▽	▼    △ bd
N.D.J	▼    △	▲    ▽ cd	▼    ▽	▲    △ dd
E.Q.X	▼    △	▼    ▽ ed	▼    ▽	▼    △ fd

Afternoon

Hemisp. Season	210~285		285~360	
	North	South	North	South
M.J.J	▲    ▽	▼    △ gd	▲    △	▼    ▽ hd
N.D.J	▼    ▽	▲    △ id	▼    △	▲    ▽ Jd
E.Q.X	▼    ▽	▼    △ kd	▼    △	▼    ▽ Ld

Table 3 Effect of meridional and zonal winds on the Ne at 600 km. ▲ and ▼ shows the upward (downward) motions of ions caused by meridional wind Δ and ▽ show the upward (downward) motion caused by zonal wind.

The same direction of black and white arrows in the Table 3 indicate that both zonal and meridional winds drive plasma in the same direction and, therefore, enhances the increase of electron density or the decrease, depending on the angle between geomagnetic field and neutral wind direction.

In the morning hours two cases exist, (**ad** and **dd**) of Table 3, where both meridional and zonal winds drive plasma in the same direction. The first one, denoted as **ad** in the column is northern summer season in the longitude zone of 210-285, where plasma is pushed up in the northern hemisphere and pushed down in the southern hemisphere. As a result plasma density increases in the northern hemisphere and reduces in the southern hemisphere. Therefore it is predicted that difference of Ne between northern hemisphere and southern hemisphere becomes the highest in the morning in May, June and July in 210-285 longitude .



The second case, denoted as **dd** is N.D.J season in the longitude zone of 285-360, where both zonal and meridional winds push the plasma down in the northern hemisphere and push it upward in the southern hemisphere.

For afternoon hours, two cases exist where both zonal and meridional winds drive plasma in the same direction (columns **id** and **hd**) and difference of Ne between both hemispheres should be enhanced. The first case denoted as **id** in the longitude zone of 210-285, where plasma is pushed down in northern hemisphere, and pushed up in the southern hemisphere by both winds. The second case, denoted as **hd** occurs in M.J.J season in the longitude zone of 285-360. The plasma is pushed up in the northern hemisphere and pushed down in the southern hemisphere. In other columns (**bd**, **cd**, **ed**, and **fd** for the morning overshoot and **gd**, **jd**, **kd**, and **ld** for the afternoon overshoot), two neutral wind components suppress the effect each other.

## 5. Solar activity dependence of Te/Ne profile

In order to see the solar activity dependence of Te/Ne, we have grouped Te/Ne data into two solar flux levels, (a) F10.7 flux is less than 200 and (b) when it is larger than 200. As shown in Figures 7 and 8 for Ne and Te, respectively, Te is sensitive even to a slight variation of electron density, which is produced by the difference of solar flux intensity. In Figures 10 and 11, we have plotted the Ne/Te variations for three seasons (M.J.J, N.D.J and E.Q.X) including all longitudes. Two features are seen clearly from these figures. First, the morning overshoot is enhanced over equator for larger solar flux especially for two seasons, N.D.J and M.J.J. During the equinox period, the morning overshoot is less remarkable than other two seasons (Oyama et al., 1996b). The second feature is that the difference between northern and southern hemispheres becomes larger as solar flux increases.

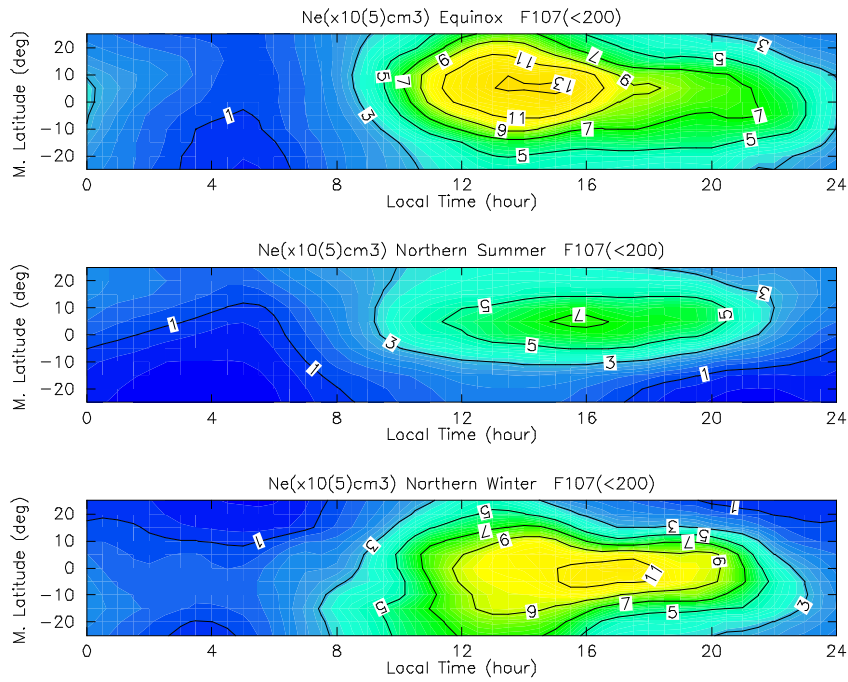


Figure 11(a). Local time variation of Ne for the solar flux, F10.7 smaller than 200 for three seasons: from the top to the bottom of each figures, equinox, northern summer, and northern winter.

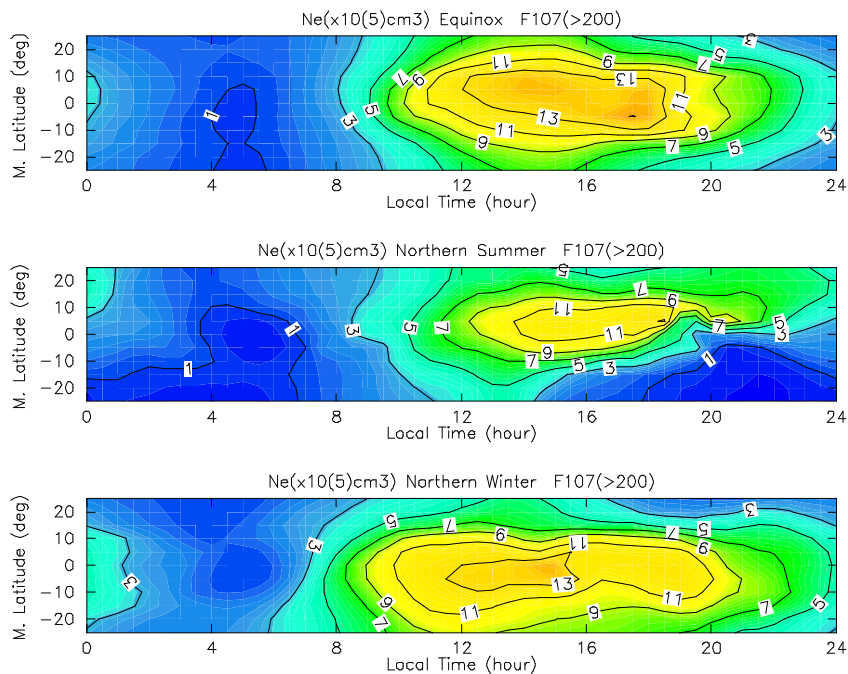


Figure 11(b). The same as Figure 7(a) but for F10.7 larger than 200.

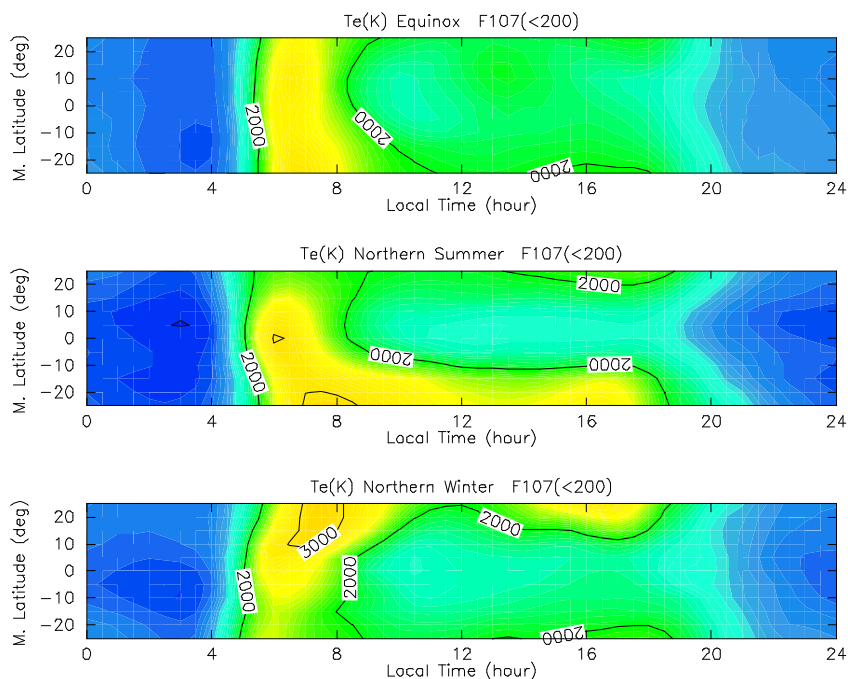


Figure 12(a). Local time variation of Te for solar flux less than 200 for three seasons: from the top to the bottom of each figures, equinox, northern summer, and northern winter.

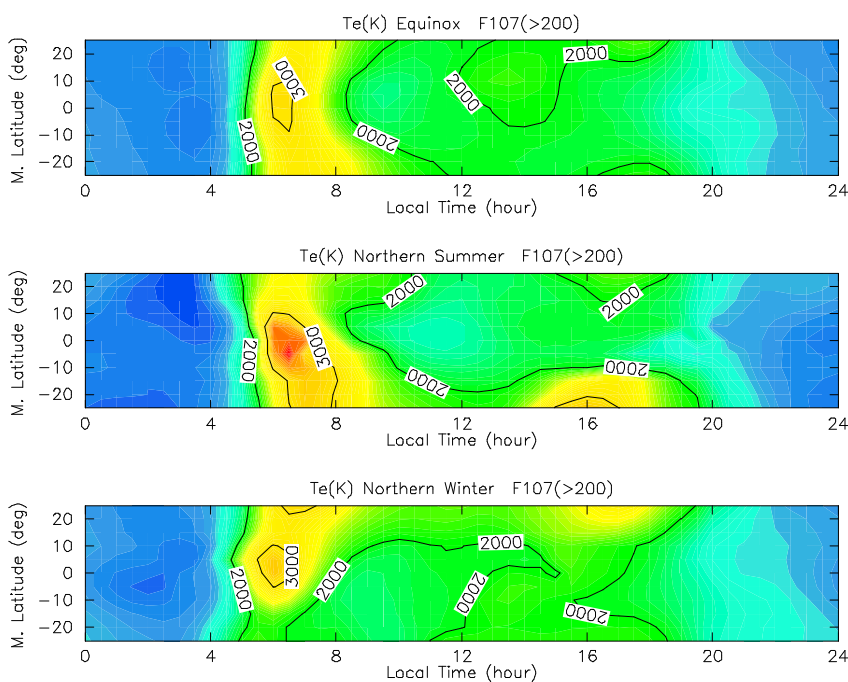


Figure.12 (b). The same as Figure 8 (a) but for F10.7 larger than 200.



## 6. Discussion

We discuss the behavior of Te and Ne, by using Tables 2 and 3. During the morning overshoot period, in the longitude zone of 210-285, according to the column (et), Te in the southern hemisphere is 230 K higher than in the northern hemisphere in the E.Q.X season, although both hemispheres should be symmetric from the point of the solar energy absorption in the ionosphere. The difference can be explained by the zonal wind, which blows from east to west in the morning. As one can understand from table 3, plasma density in the northern hemisphere increases and decreases in the southern hemisphere and as a result Te decreases in the northern hemisphere and increases in the southern hemisphere, as Te is inversely proportional to Ne during daytime. Te of M.J.J (N.D.J) season which is higher (lower) in northern (southern) hemisphere than in southern (northern) hemisphere is qualitatively understood by the meridional wind. Difference of Te (3140K - 2170 K) between northern and southern hemispheres in M.J.J season, which is larger than N.D.J season (column ct), might be explained as a result of the combined effect of meridional and zonal components.

In the longitude range of 285-360, in E.Q.X season (where Te should be the same if no zonal wind component exist), Te of the northern hemisphere which is 300 K higher than in northern hemisphere (column ft) can be explained by the effect of zonal wind which hits the magnetic meridian tilting it toward west as about 10 degrees larger than in 210-285 longitude region. Nearly equal Te between northern and southern hemispheres in M.J.J season (column bt) suggests that the effect of zonal wind is strong enough to cancel the meridional wind effect. Large difference of Te between two hemispheres in N.D.J season (column dt) is consistent with the enhanced combination of zonal and meridional wind components.

For the afternoon overshoot in the longitude range of 210-285, nearly equal Te between northern and southern hemispheres in the E.Q.X season (column kt) suggests that in the afternoon zonal component is smaller than in the morning. In N.D.J season (column it) Te in the northern hemisphere is higher than in the southern hemisphere, which is consistent from the point of wind direction. Te behavior in M.J.J season (gt) is understood from table 3 as due to meridional wind component mainly.

In the longitude zone of 285-360, in the E.Q.X season the difference of northern / southern hemispheres is 130 K (column lt), which is 170 K lower than the difference of Te in the E.Q.X morning



overshoot (**ft**) This again suggests that zonal wind is weak in the afternoon as we suggested from column **kt**.

In contrast to the E.Q.X season, the  $T_e$  in N.D.J season (column **jt**) is nearly the same between two hemispheres, which means that zonal wind effect is strong enough to cancel meridional wind effect. Big difference of  $T_e$  between two hemispheres (**ht**) which is intensified as a combined result of meridional and zonal wind effects supports the above statement.

From the description above, the following statement can be drawn; (1) meridional wind component produces the  $T_e$  difference between two hemispheres, (2) effects of declination of the magnetic meridional plane on  $T_e$  is detectable, especially, in the 285-360 longitude. (3). zonal wind during M.J.J and N.D.J season (column **it**, and **ht**) is stronger than in E.Q.X and in the E.Q.X, west to east wind which blows in the afternoon is weaker than the east to west wind in the morning.

The fact that the difference of  $T_e$  between two hemispheres is enhanced at higher solar activity suggests that meridional neutral wind blows more intensely in higher solar flux period.

## 7. Conclusions

Diurnal, latitudinal, and longitudinal variations of  $T_e/N_e$  in the equatorial ionosphere at 600 km during daytime are discussed. Even a small difference of both parameters in two different longitude zones 210-285 and 285-360, where magnetic meridional plane tilts eastward and westward, respectively, are explained by the effect of neutral wind. Especially the effect of zonal wind is almost comparable to the effect of meridional wind in the longitude zone of 285-360. Present study suggests the possibility to calculate thermospheric neutral wind system from the  $T_e/N_e$  data (Su et al., 1995). The  $T_e$  data set which was used here are available from NSSDC.



## References

- Balan, K.-I. Oama, G.J. Bailey, S. Fukao, S. Watanabe, N.A. Abdu .A plasma temperature anomaly in the equatorial ionosphere. *J. Geophys. Res.*, 102, 7485-7492, 1997.
- Cooke D., C.Roth, H.Luehr, N.Jakowsky. In situ plasma observation at 400km on the CHAMP satellite. EGS meeting, 2003.
- Dabas, R.S., M.Reddy, K.-I.Oyama .Study of anomalous electron temperature variation in the topside ionosphere using HINOTORI satellite. *J. Atmos. Terr. Phys.*, 62, 1351-1359, 2000.
- Hedin, A.E., M.A.Biondi, R.G.Burnside, G.Hernandez, R.M.Johnson, T.L.Killeen, C.Mazaudier, J.W.Meriwether, J.E.Salah, R.J.Sica, R.W.Smith, N.W.Spencer, V.B.Wickwar, and T.S.Virdi. Revised Global model of thermosphere winds using satellite and ground -based observations. *J. Geophys. Res.* **96**, A5, 7657-7688, 1991.
- Oyama K.-I. and K.Schlegel. Temperature structure of plasma bubbles in the lower latitude ionosphere around 600Km altitude. *Planet.Space.Sci.*, **36**, (6)553-567, 1988.
- Oyama, K.-I. Electron temperature measurements carried out by Japanese scientific satellites. *Adv.Space. Res.*, 11, (10)149-(10)158, 1991.
- Oyama, K.-I., S.Watanabe, and H.Oya. Energetics of the plasma bubble. *Adv.Space Res.*, **13**, (1)293-(1)297, 1993.
- Oyama K.-I. Verification of IRI plasma temperature at great altitude by satellite data. *Adv. Space Res.*, **14**, (12)105-(12)113, 1994.
- Oyama K.-I., S.Watanabe, Y.Z.Su, T.Takahashi, K. Hirao. Season local time, and longitudinal variations of electron temperature at the height of  $\sim 600$ Km in the low latitude region. *Adv. Space Res.*, **18**(6), 269-278, 1996a.
- Oyama K.-I., N. Balan, S. Watanabe, T. Takahashi, F. Isoda, G.J. Baily, H. Oya. Morning overshoot of  $T_e$  enhanced by downward plasma drift in the equatorial topside ionosphere. *J. Geomag. Geoelectr.*, **48**, 959-966, 1996b.
- Oyama, K.-I., T.Abe, K.Schlegel, A.Nagy, J.Kim, and K.Marubashi. Electron temperature measurement in Martian ionosphere. *Earth and Planetary Sci.*, 51, 1309-1317, 1999.
- Schlegel, K., K.-I. Oyama, T.Takahashi. Global morphology of plasma bubbles in the lower ionosphere. AGARD Conference proceedings, No.44, 8/1-8/5, 1989.
- Spencer, K., and R.Plugge. Empirical model of global electron temperature distribution between 300 and 700 km based on data from AEROS-A. *J. Geophys.* **46**, 43-56, 1979.



Su Y.Z.,K.-I.Oyama, and G.J. Bailey. Comparison of satellite electron density and temperature measurements at low latitudes with a plasmasphere-ionosphere model. *J. Geophys Res.*,**100**,14591-14604, 1995.

Su Y.Z.,K.-I.Oyama, and G.J. Bailey. Longitudinal variation of the topside ionosphere at low latitudes : Satellite measurements and mathematical modellings. *J.Geophys Res.*, **101**,17191-17205, 1996a.

Su Y.Z.,K.-I.Oyama, and G.J. Bailey, T.Takahashi, S.Watanabe. Spatial and temporal variation of the electron temperature at equatorial anomaly latitudes. *Adv. Space Res.*,**18**(6),83-86, 1996b.

Torr.D.G. and M.R.Torr. Chemistry of the thermosphere and ionosphere.*J.Atmos.Terr.Phys.*,**41**,797-839, 1979.

Takahashi T., H. Oya, and S.Watanabe. Ionospheric disturbances induced by substorm associated electric field in the low latitude F region. *J.Geomag .Goelectr.*,**39**,187-209, 1987.

Watanabe.S., and H.Oya . Occurrence characteristics of low latitude ionosphere irregularities observed by impedance probe on board the HINOTORI satellite. *J.Geomag.Goelectr.*,**38**,125-150, 1986.

Watanabe S.,K.-I. Oyama, and M.A .Abdu . A computer simulation of electron and ion densities and temperatures in the equatorial F region and comparison with HINOTORI results. *J. Geophys. Res.*, **100**,14581-14590, 1995a.

Watanabe S., T. Takahashi, H. Oya, K.-I. Oyama., Table of electron density at 600Km altitude during 1981-1982. First step towards IRI revisions, ISAS, RN579, 1995b.